Journal of Advanced Research (2015) **6**, 587–592

Cairo University

**Journal of Advanced Research**

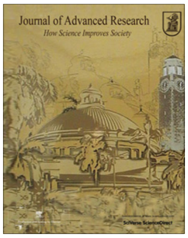

ORIGINAL ARTICLE

# A unified classification model for modeling of seismic liquefaction potential of soil based on CPT

**Pijush Samui** [a,*], **R. Hariharan** [b]

[a] *Centre for Disaster Mitigation and Management, VIT University, Vellore 632014, India*
[b] *Annai Mira College of Engineering and Technology, Department of Computer Science, Arapakam, Vellore 632517, India*

ARTICLE INFO

*Article history:*
Received 31 August 2013
Received in revised form 5 February 2014
Accepted 6 February 2014
Available online 14 February 2014

*Keywords:*
Liquefaction
Cone Penetration Test
Minimax Probability Machine
Artificial Intelligence

ABSTRACT

The evaluation of liquefaction potential of soil due to an earthquake is an important step in geosciences. This article examines the capability of Minimax Probability Machine (MPM) for the prediction of seismic liquefaction potential of soil based on the Cone Penetration Test (CPT) data. The dataset has been taken from Chi–Chi earthquake. MPM is developed based on the use of hyperplanes. It has been adopted as a classification tool. This article uses two models (MODEL I and MODEL II). MODEL I employs Cone Resistance ($q_c$) and Cyclic Stress Ratio (CSR) as input variables. $q_c$ and Peak Ground Acceleration (PGA) have been taken as inputs for MODEL II. The developed MPM gives 100% accuracy. The results show that the developed MPM can predict liquefaction potential of soil based on $q_c$ and PGA.

## Introduction

Liquefaction causes lot of damages during earthquake. So, the prediction of liquefaction potential of soil due to an earthquake is an important step for earthquake hazard mitigation. There are various techniques available for the determination of liquefaction potential of soil in the literature [1–13]. However, available methods have some limitations [14]. Researchers used Artificial Intelligence (AI) techniques for the prediction of liquefaction susceptibility of soil [14–25].

This article adopts Cone Penetration Test (CPT) based Minimax Probability Machine (MPM) for the prediction of seismic liquefaction potential of soil. The datasets have been collected from Chi–Chi earthquake at Taiwan. MPP is developed by Lanckriet et al. [26]. MPM is constructed in probabilistic framework. This article uses MPM as a classification problem. It has been successfully adopted for modeling different problems in engineering [27–29]. The magnitude of earthquake was 7.6. The epicenter of earthquake was at 23.87°N and 120.75E [30]. Extensive liquefaction was observed at Yuanlin, Wufeng, and Nantou. Many CPT tests were conducted after the earthquake [30]. Two models (MODEL I and MODEL II) have been used to get best performance. MODEL I adopts Cone Resistance ($q_c$) and Cyclic Stress Ratio (CSR) as input variables. $q_c$ and Peck Ground Acceleration

---

[*] Corresponding author. Tel.: +91 416 2202281; fax: +91 416 2243092.
E-mail address: pijush.phd@gmail.com (P. Samui).
Peer review under responsibility of Cairo University.

Production and hosting by Elsevier

2090-1232
http://dx.doi.org/10.1016/j.jare.2014.02.002

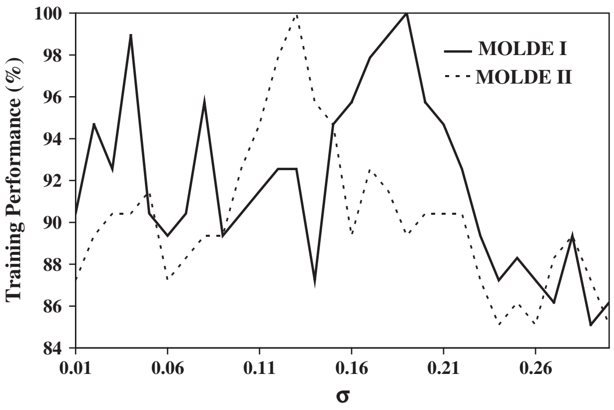

**Fig. 1** Effect of $\sigma$ on training performance (%).

**Table 1** Performance of training dataset.

| $q_c$ (MPa) | PGA(gal) | CSR | Actual class | Predicted class | |
|---|---|---|---|---|---|
| | | | | MODEL I | MODEL II |
| 1.27 | 774 | 0.643 | −1 | −1 | −1 |
| 0.72 | 774 | 0.665 | −1 | −1 | −1 |
| 1.35 | 774 | 0.802 | −1 | −1 | −1 |
| 11.66 | 774 | 0.836 | 1 | 1 | 1 |
| 13.89 | 774 | 0.853 | 1 | 1 | 1 |
| 20.05 | 774 | 0.826 | 1 | 1 | 1 |
| 0.94 | 420 | 0.34 | −1 | −1 | −1 |
| 1.47 | 420 | 0.37 | −1 | −1 | −1 |
| 11.56 | 420 | 0.37 | 1 | 1 | 1 |
| 12.89 | 420 | 0.46 | 1 | 1 | 1 |
| 16.3 | 420 | 0.43 | 1 | 1 | 1 |
| 1.41 | 420 | 0.35 | −1 | −1 | −1 |
| 11.96 | 420 | 0.46 | 1 | 1 | 1 |
| 1.87 | 420 | 0.42 | −1 | −1 | −1 |
| 5.77 | 420 | 0.48 | −1 | −1 | −1 |
| 2.54 | 188 | 0.17 | −1 | −1 | −1 |
| 7.46 | 188 | 0.22 | 1 | 1 | 1 |
| 7.62 | 188 | 0.22 | 1 | 1 | 1 |
| 8.03 | 188 | 0.21 | 1 | 1 | 1 |
| 7.02 | 188 | 0.2 | 1 | 1 | 1 |
| 7.72 | 188 | 0.22 | 1 | 1 | 1 |
| 7.68 | 188 | 0.18 | 1 | 1 | 1 |
| 2.22 | 188 | 0.2 | −1 | −1 | −1 |
| 12.15 | 188 | 0.2 | 1 | 1 | 1 |
| 2.54 | 188 | 0.16 | −1 | −1 | −1 |
| 8.15 | 188 | 0.21 | 1 | 1 | 1 |
| 10.08 | 188 | 0.21 | 1 | 1 | 1 |
| 12.43 | 188 | 0.2 | 1 | 1 | 1 |
| 1.62 | 188 | 0.16 | −1 | −1 | −1 |
| 2.45 | 188 | 0.19 | −1 | −1 | −1 |
| 6.7 | 188 | 0.21 | 1 | 1 | 1 |
| 13.65 | 188 | 0.2 | 1 | 1 | 1 |
| 17.08 | 188 | 0.2 | 1 | 1 | 1 |
| 2.66 | 188 | 0.18 | −1 | −1 | −1 |
| 8.25 | 188 | 0.21 | 1 | 1 | 1 |
| 7.41 | 188 | 0.21 | 1 | 1 | 1 |
| 2.54 | 188 | 0.2 | −1 | −1 | −1 |
| 12.77 | 188 | 0.2 | 1 | 1 | 1 |
| 1.18 | 188 | 0.16 | −1 | −1 | −1 |
| 2.96 | 188 | 0.2 | −1 | −1 | −1 |
| 8 | 188 | 0.2 | 1 | 1 | 1 |
| 8.74 | 188 | 0.19 | 1 | 1 | 1 |
| 11.26 | 188 | 0.17 | 1 | 1 | 1 |
| 7.52 | 207 | 0.23 | 1 | 1 | 1 |
| 6.61 | 188 | 0.22 | 1 | 1 | 1 |
| 8.3 | 188 | 0.2 | 1 | 1 | 1 |
| 8.32 | 188 | 0.21 | 1 | 1 | 1 |
| 3 | 188 | 0.18 | −1 | −1 | −1 |
| 2.09 | 188 | 0.2 | −1 | −1 | −1 |
| 2.78 | 188 | 0.24 | −1 | −1 | −1 |
| 3.05 | 188 | 0.22 | −1 | −1 | −1 |
| 14.67 | 188 | 0.2 | 1 | 1 | 1 |
| 10.61 | 188 | 0.2 | 1 | 1 | 1 |
| 13.65 | 188 | 0.19 | 1 | 1 | 1 |
| 1.28 | 121 | 0.13 | −1 | −1 | −1 |
| 0.64 | 121 | 0.13 | −1 | −1 | −1 |
| 5.16 | 121 | 0.14 | 1 | 1 | 1 |
| 3.26 | 121 | 0.11 | −1 | −1 | −1 |
| 7.4 | 121 | 0.14 | 1 | 1 | 1 |
| 7.04 | 121 | 0.15 | 1 | 1 | 1 |
| 7.47 | 121 | 0.15 | 1 | 1 | 1 |
| 6.54 | 121 | 0.14 | 1 | 1 | 1 |
| 6.64 | 121 | 0.14 | 1 | 1 | 1 |
| 5.59 | 121 | 0.15 | 1 | 1 | 1 |
| 6.85 | 121 | 0.14 | 1 | 1 | 1 |
| 6.68 | 121 | 0.14 | 1 | 1 | 1 |
| 5.21 | 121 | 0.14 | 1 | 1 | 1 |
| 7.18 | 121 | 0.14 | 1 | 1 | 1 |
| 5.91 | 121 | 0.15 | 1 | 1 | 1 |
| 5.38 | 121 | 0.15 | 1 | 1 | 1 |
| 7.99 | 121 | 0.14 | 1 | 1 | 1 |
| 7.38 | 121 | 0.14 | 1 | 1 | 1 |
| 7.41 | 121 | 0.14 | 1 | 1 | 1 |
| 6.73 | 121 | 0.15 | 1 | 1 | 1 |
| 6.49 | 121 | 0.14 | 1 | 1 | 1 |
| 5.47 | 121 | 0.14 | 1 | 1 | 1 |
| 0.92 | 121 | 0.11 | −1 | −1 | −1 |
| 1.5 | 121 | 0.13 | −1 | −1 | −1 |
| 6.05 | 121 | 0.15 | 1 | 1 | 1 |
| 6.76 | 121 | 0.15 | 1 | 1 | 1 |
| 2.49 | 121 | 0.12 | −1 | −1 | −1 |
| 1.89 | 121 | 0.14 | −1 | −1 | −1 |
| 1.54 | 121 | 0.14 | −1 | −1 | −1 |
| 7.43 | 121 | 0.14 | 1 | 1 | 1 |
| 6.61 | 121 | 0.14 | 1 | 1 | 1 |
| 7.12 | 121 | 0.14 | 1 | 1 | 1 |
| 6.08 | 121 | 0.14 | 1 | 1 | 1 |
| 9.48 | 121 | 0.12 | 1 | 1 | 1 |
| 0.2 | 121 | 0.12 | −1 | −1 | −1 |
| 5.93 | 121 | 0.13 | 1 | 1 | 1 |
| 7.57 | 121 | 0.14 | 1 | 1 | 1 |
| 7.24 | 121 | 0.14 | 1 | 1 | 1 |
| 6.21 | 121 | 0.14 | 1 | 1 | 1 |
| 8.83 | 121 | 0.14 | 1 | 1 | 1 |

(PGA) have been used as inputs of the MODEL II. The database has been collected from the work of Ku et al. [31]. In this database, liquefaction is observed in 46 sites. The remaining 88 sites are non-liquefied. The developed MPM has been applied for the global data [16]. This article gives charts for classifying liquefiable and non-liquefiable soil.

**Table 2** Performance of testing dataset.

| $q_c$ (MPa) | PGA(gal) | CSR | Actual class | Predicted class | |
|---|---|---|---|---|---|
| | | | | MODEL I | MODEL II |
| 1.79 | 774 | 0.749 | −1 | −1 | −1 |
| 14.45 | 774 | 0.829 | 1 | 1 | 1 |
| 11.32 | 420 | 0.46 | 1 | 1 | 1 |
| 6.01 | 420 | 0.4 | −1 | −1 | −1 |
| 0.9 | 420 | 0.39 | −1 | −1 | −1 |
| 8.27 | 188 | 0.21 | 1 | 1 | 1 |
| 2.7 | 188 | 0.18 | −1 | −1 | −1 |
| 6.67 | 188 | 0.22 | 1 | 1 | 1 |
| 6.23 | 188 | 0.21 | 1 | 1 | 1 |
| 2.62 | 188 | 0.18 | −1 | −1 | −1 |
| 16.89 | 188 | 0.2 | 1 | 1 | 1 |
| 9.19 | 188 | 0.21 | 1 | 1 | 1 |
| 1.82 | 188 | 0.19 | −1 | −1 | −1 |
| 8.3 | 188 | 0.21 | 1 | 1 | 1 |
| 1.73 | 207 | 0.21 | −1 | −1 | −1 |
| 10.05 | 188 | 0.18 | 1 | 1 | 1 |
| 2.61 | 188 | 0.19 | −1 | −1 | −1 |
| 11.58 | 188 | 0.2 | 1 | 1 | 1 |
| 2.69 | 188 | 0.22 | −1 | −1 | −1 |
| 14.74 | 188 | 0.19 | 1 | 1 | 1 |
| 5.46 | 121 | 0.14 | 1 | 1 | 1 |
| 2.65 | 121 | 0.13 | −1 | −1 | −1 |
| 7.68 | 121 | 0.14 | 1 | 1 | 1 |
| 7.58 | 121 | 0.14 | 1 | 1 | 1 |
| 6.12 | 121 | 0.14 | 1 | 1 | 1 |
| 6.62 | 121 | 0.15 | 1 | 1 | 1 |
| 7.03 | 121 | 0.14 | 1 | 1 | 1 |
| 6.32 | 121 | 0.14 | 1 | 1 | 1 |
| 0.64 | 121 | 0.13 | −1 | −1 | −1 |
| 2.01 | 121 | 0.13 | −1 | −1 | −1 |
| 7.72 | 121 | 0.14 | 1 | 1 | 1 |
| 7.76 | 121 | 0.14 | 1 | 1 | 1 |
| 7.94 | 121 | 0.14 | 1 | 1 | 1 |
| 0.18 | 121 | 0.12 | −1 | −1 | −1 |
| 1.97 | 774 | 0.665 | −1 | −1 | −1 |
| 3.86 | 420 | 0.37 | −1 | −1 | −1 |
| 6.8 | 188 | 0.21 | 1 | 1 | 1 |
| 8.01 | 188 | 0.2 | 1 | 1 | 1 |
| 0.23 | 121 | 0.11 | −1 | −1 | −1 |
| 6.83 | 207 | 0.23 | 1 | 1 | 1 |

## Details of MPM

In MPM, it is assumed that positive definite covariance matrices exist in each of the two classes. In MPM, the probability of misclassification of future data is minimized [26]. In MPM, following optimal hyperplane is used for separating the two classes of points.

$$a^T z = b \quad a, z \in R^n; \quad b \in R \tag{1}$$

In MPM, the following optimization problem is constructed [20]:

$$\max_{\alpha, b, a \neq 0} \alpha \quad \text{Constraint :} \quad \begin{array}{l} \inf P_r\{a^T x \geq b\} \geqslant \alpha \\ \inf P_r\{a^T y \leq b\} \geqslant \alpha \end{array} \tag{2}$$

where $\alpha$ is called the worst-case accuracy.

The above optimization problem (2) is solved by Lagrangian Multiplier. So, it takes the following form.

**Table 3** Performance of the global data [16].

| Site | $q_c$ (MPa) | PGA (g) | Actual class | Predicted class |
|---|---|---|---|---|
| Kawagishicho | 3.2 | 0.16 | −1 | 1 |
| Kawagishicho | 1.6 | 0.16 | −1 | −1 |
| Kawagishicho | 7.2 | 0.16 | −1 | −1 |
| Kawagishicho | 5.6 | 0.16 | −1 | −1 |
| Kawagishicho | 5.45 | 0.16 | −1 | 1 |
| Kawagishicho | 8.84 | 0.16 | −1 | −1 |
| Kawagishicho | 9.7 | 0.16 | −1 | −1 |
| Kawagishicho | 8 | 0.16 | 1 | 1 |
| Kawagishicho | 14.55 | 0.16 | 1 | 1 |
| Noshirocho | 10 | 0.23 | 1 | −1 |
| Noshirocho | 16 | 0.23 | 1 | 1 |
| Noshirocho | 15.38 | 0.23 | 1 | 1 |
| Noshirocho | 1.79 | 0.23 | −1 | −1 |
| Noshirocho | 4.1 | 0.23 | −1 | −1 |
| Noshirocho | 7.95 | 0.23 | −1 | −1 |
| Noshirocho | 8.97 | 0.23 | −1 | −1 |
| T-10 | 1.7 | 0.4 | −1 | −1 |
| T-10 | 9.4 | 0.4 | −1 | 1 |
| T-10 | 5.7 | 0.4 | −1 | 1 |
| T-10 | 7.6 | 0.4 | −1 | −1 |
| T-11 | 1.5 | 0.4 | −1 | −1 |
| T-11 | 1 | 0.4 | −1 | 1 |
| T-11 | 5 | 0.4 | −1 | −1 |
| T-12 | 2.5 | 0.4 | −1 | −1 |
| T-12 | 2.6 | 0.4 | −1 | −1 |
| T-12 | 3.2 | 0.4 | −1 | −1 |
| T-12 | 5.8 | 0.4 | −1 | 1 |
| T-12 | 3.5 | 0.4 | −1 | −1 |
| T-12 | 8.4 | 0.4 | −1 | −1 |
| T-13 | 1.7 | 0.4 | −1 | 1 |
| T-13 | 3.5 | 0.4 | −1 | −1 |
| T-13 | 4.1 | 0.4 | −1 | −1 |
| T-14 | 5.5 | 0.4 | −1 | −1 |
| T-14 | 9 | 0.4 | −1 | 1 |
| T-15 | 7 | 0.4 | −1 | −1 |
| T-15 | 1.18 | 0.4 | −1 | −1 |
| T-15 | 4.24 | 0.4 | −1 | −1 |
| T-16 | 11.47 | 0.4 | 1 | 1 |
| T-16 | 15.76 | 0.4 | 1 | 1 |
| T-17 | 11.39 | 0.2 | 1 | 1 |
| T-17 | 12.12 | 0.2 | 1 | 1 |
| T-17 | 17.76 | 0.2 | 1 | −1 |
| T-23 | 2.65 | 0.2 | −1 | 1 |
| T-24 | 4.4 | 0.2 | −1 | −1 |
| T-24 | 3 | 0.2 | −1 | −1 |
| T-25 | 9 | 0.2 | −1 | 1 |
| T-26 | 2 | 0.1 | −1 | −1 |
| T-27 | 1.1 | 0.2 | −1 | −1 |
| T-28 | 15.5 | 0.1 | 1 | 1 |
| T-28 | 6.5 | 0.1 | 1 | 1 |
| T-29 | 9 | 0.1 | 1 | 1 |
| T-29 | 2.5 | 0.1 | 1 | 1 |
| T-29 | 16.5 | 0.1 | 1 | 1 |
| T-30 | 13.65 | 0.1 | 1 | 1 |
| L-1 | 8.47 | 0.2 | 1 | −1 |
| L-1 | 4.55 | 0.2 | 1 | 1 |
| L-1 | 5.79 | 0.2 | 1 | −1 |
| L-2 | 2.48 | 0.2 | −1 | −1 |
| L-2 | 1.57 | 0.2 | −1 | −1 |
| L-2 | 1.45 | 0.2 | −1 | −1 |
| L-2 | 2.15 | 0.2 | −1 | −1 |
| L-2 | 2.6 | 0.2 | −1 | −1 |

**Table 3** (*continued*)

| Site | $q_c$ (MPa) | PGA (g) | Actual class | Predicted class |
|---|---|---|---|---|
| L-3 | 2.73 | 0.2 | −1 | 1 |
| L-3 | 1.78 | 0.2 | −1 | −1 |
| L-5 | 7.64 | 0.2 | 1 | 1 |
| Heber Road | 25.6 | 0.8 | 1 | 1 |
| A1 | 24.7 | 0.8 | 1 | 1 |
| A1 | 31.4 | 0.8 | 1 | 1 |
| A2 | 1.43 | 0.8 | −1 | −1 |
| A2 | 2.48 | 0.8 | −1 | 1 |
| A3 | 4.03 | 0.8 | −1 | −1 |
| A3 | 3.3 | 0.8 | 1 | 1 |
| A4 | 8.8 | 0.8 | 1 | 1 |
| A4 | 6.7 | 0.8 | 1 | 1 |
| T-18 | 1.65 | 0.2 | −1 | −1 |
| T-18 | 3.65 | 0.2 | −1 | −1 |
| T-19 | 1.03 | 0.2 | −1 | −1 |
| T-19 | 5 | 0.2 | −1 | −1 |
| T-19 | 2.91 | 0.2 | −1 | −1 |
| T-19 | 6.06 | 0.2 | −1 | −1 |
| T-20 | 13.24 | 0.2 | 1 | 1 |
| T-20 | 13.06 | 0.2 | 1 | −1 |
| T-20 | 16.59 | 0.2 | 1 | 1 |
| T-21 | 10.59 | 0.2 | 1 | 1 |
| T-21 | 9.12 | 0.2 | 1 | 1 |
| T-21 | 11.29 | 0.2 | 1 | 1 |
| T-22 | 1.94 | 0.2 | −1 | −1 |
| T-22 | 5 | 0.2 | −1 | −1 |
| T-23 | 2.24 | 0.2 | −1 | −1 |
| T-30 | 14.12 | 0.1 | 1 | 1 |
| T-30 | 18.94 | 0.1 | 1 | 1 |
| T-31 | 3.52 | 0.2 | −1 | −1 |
| T-31 | 2.73 | 0.2 | −1 | −1 |
| T-32 | 3.29 | 0.2 | −1 | 1 |
| T-32 | 4.12 | 0.2 | −1 | −1 |
| T-32 | 2.94 | 0.2 | −1 | −1 |
| T-33 | 3 | 0.2 | −1 | −1 |
| T-33 | 5.85 | 0.2 | −1 | −1 |
| T-33 | 9 | 0.2 | −1 | −1 |
| T-34 | 1.8 | 0.2 | −1 | −1 |
| T-35 | 2.55 | 0.2 | −1 | −1 |
| T-35 | 4.5 | 0.2 | −1 | −1 |
| T-35 | 4.24 | 0.2 | −1 | −1 |
| T-36 | 8 | 0.2 | 1 | 1 |
| Dimbovitza site | 5.22 | 0.22 | −1 | 1 |
| Dimbovitza site | 3.73 | 0.22 | −1 | −1 |
| Dimbovitza site | 3.11 | 0.22 | −1 | −1 |
| Dimbovitza site | 1.32 | 0.22 | −1 | −1 |
| Dimbovitza site | 5.22 | 0.22 | −1 | −1 |

$$\max_{\kappa,a} \quad \kappa \quad \text{Constraint}: \begin{array}{l} -b + a^T x \geqslant \kappa \sqrt{a^T \sum_x a} \\ -b - a^T y \geqslant \kappa \sqrt{a^T \sum_y a} \end{array} \tag{3}$$

The optimization problem (3) is written in the following form:

$$\min_a \sqrt{a^T \sum_y a} + \lambda \sqrt{a^T \sum_x a}$$

$$\text{Subjected to}: a^T(x - y) = 1 \tag{4}$$

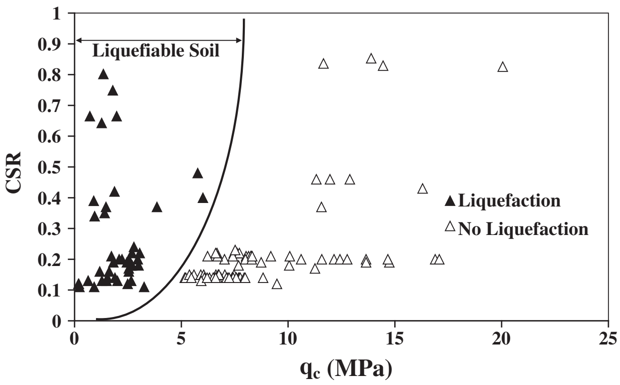

**Fig. 2** Plot between CSR and $q_c$.

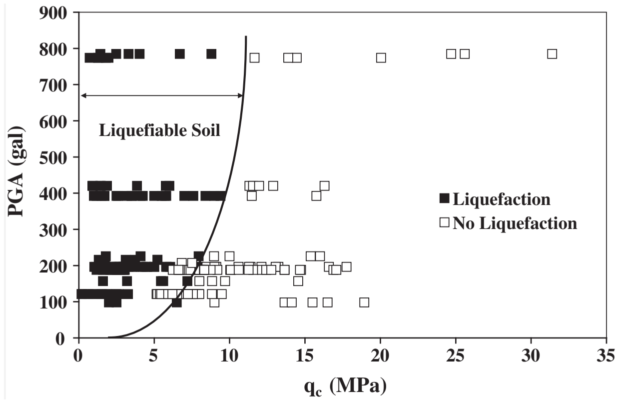

**Fig. 3** Plot between PGA and $q_c$.

The above optimization problem (4) is solved by convex programming technique.

To develop the above MPM, non-liquefied sites are denoted by +1 and liquefied sites are denoted by −1. In MPM, training dataset is adopted to develop the model and a testing is employed to verify the developed MPM. Ninety-four datasets have been adopted as training datasets. The 40 remaining datasets have been employed as testing datasets.

In this article, the datasets are scaled between 0 and 1. This study adopts radial basis function ($K(x_i, x) = \exp\left[\frac{-(x_i - x)(x_i - x)^T}{2\sigma^2}\right]$) (where $\sigma$ is width of radial basis function) as kernel function for developing the MPM. This article employs MATLAB software for constructing MPM.

## Results and discussion

The success of MPM depends on the choice of proper value of $\sigma$. This study adopts trial and error approach for the determination of the design value of $\sigma$. Training and testing performance have been determined by using the following equation.

$$\text{Training/Testing performance}(\%) = \left(\frac{\text{No of data predicted accurately by MPM}}{\text{Total data}}\right) \times 100 \tag{5}$$

Fig. 1 shows the effect of $\sigma$ on training performance (%) for MODEL I. It is observed from Fig. 1 that the developed MPM gives best training performance at $\sigma$ = 0.19 for

MODEL I. The developed MPM gives 100% training performance. The performance of testing dataset is also 100%. Tables 1 and 2 illustrate the performance of MPM for training and testing dataset respectively. The classification of MPM has been plotted in Fig. 2.

For MODEL II, the effect of $\sigma$ on training performance has been shown in Fig. 1. It is clear from Fig. 2 that the best training performance has been achieved at $\sigma = 0.13$. The developed MPM produces 100% training as well as testing performance. So, the developed MODEL II gives same performance as given by MODEL II. The performance of MPM for training and testing dataset has been depicted in Tables 1 and 2, respectively.

Fig. 3 plots the results of MODEL II. The generalization capability of developed MODEL II has been examined by the global datasets [16]. These global datasets consists information about liquefiable and non-liquefiable soil of five earthquakes. The developed MODEL II correctly classifies 100 datasets out of 109. Therefore, the developed MPM shows good generalization capability. Table 3 shows the performance of global data.

## Conclusions

This article successfully applied MPM for the determination of seismic liquefaction potential of soil. Two models (MODEL I and MODEL II) have been tried to get best performance. The performance of MPM for MODEL I and II is excellent. This study shows that the developed MPM can predict liquefaction potential of soil based on $q_c$ and PGA. Geotechnical engineers can use the developed charts for the determination of seismic liquefaction potential of soil. The developed MPM shows good generalization capability. MPM model can be adopted for modeling different problems in geosciences.

## Conflict of interest

*The authors have declared no conflict of interest.*

## Compliance with Ethics Requirements

*This article does not contain any studies with human or animal subjects.*

## References

[1] Seed HB, Idriss IM. Analysis of soil liquefaction: Niigata earthquake. J Soil Mech Found Div ASCE 1967;93(3):83–108.

[2] Seed HB, Idriss IM. Simplified procedure for evaluating soil liquefaction potential. J Soil Mech Found Div ASCE 1971;97(9):1249–73.

[3] Seed HB, Idriss IM, Arango I. Evaluation of liquefaction potential using field performance data. J Geotech Eng Div ASCE 1983;109(3):458–82.

[4] Seed HB, Tokimatsu K, Harder LF, Chung RM. Influence of SPT procedures in soil liquefaction resistance evaluation. Rep. No. UCB/EERC-84/15, Earthquake Eng Res Ctr, California: Univ. of California, Berkeley; 1984.

[5] Youd TL, Idriss IM, Andrus RD, Arango I, Castro G, Christian JT, et al. Liquefaction resistance of soils: summary report from the 1996 NCEER and 1998 NCEER/NSF workshops on evaluation of liquefaction resistance of soils. J Geotech Geoenviron Eng ASCE 2001;127(10):817–33.

[6] Robertson PK, Campanella RG. Liquefaction potential of sands using the cone penetration test. J Geotech Div ASCE 1985;111(3):384–407.

[7] Andrus RD, Stokoe KH. Liquefaction resistance of soils from shear wave velocity. J Geotech Geoenviron Eng ASCE 2000;108,126(11):1015–25.

[8] Cavallaro A, Grasso S, Maugeri M, Motta E. An innovative low-cost SDMT marine investigation for the evaluation of the liquefaction potential in the Genova Harbour (Italy). In: Proceedings of the 4th international conference on geotechnical and geophysical site characterization; 2013. ISC'4 – ISBN: 978-0-415-62136-6, At Porto de Galinhas.

[9] Maugeri M, Grasso S. Liquefaction potential evaluation at Catania Harbour (Italy). WIT Trans Built Environ 2013;132:69–81.

[10] Monaco P, Totani G, Totani F, Grasso S, Maugeri M. Site effects and site amplification due to the 2009 Abruzzo earthquake. Earthquake Resist Eng Struct 2009;VIII.

[11] Monaco P, Santucci de Magistris F, Grasso S, Marchetti S, Maugeri M, Totani G. Analysis of the liquefaction phenomena in the village of Vittorito (L'Aquila). Bull Earthquake Eng 2011;9:231–61.

[12] Grasso S, Maugeri M. The seismic microzonation of the city of Catania (Italy) for the Etna Scenario Earthquake (M6.2) of February 20 1818. Earthquake Spectra 2012;28(2):573–94.

[13] Grasso S, Maugeri M. The Seismic Dilatometer Marchetti Test (SDMT) for evaluating liquefaction potential under cyclic loading. Geotech Earthquake Eng Soil Dyn 2008;IV:1–15.

[14] Samui P. Support vector machine applied to settlement of shallow foundations on cohesionless soils. Comput Goetech 2008;35(3):419–27.

[15] Goh ATC. Seismic liquefaction potential assessed by neural network. J Geotech Geoenviron Eng 1994;120(9):1467–80.

[16] Goh ATC. Neural-network modeling of CPT seismic liquefaction data. J Geotech Eng 1996;122(1):70–3.

[17] Agrawal G, Chameau JA, Bourdeau PL. Assessing the liquefaction susceptibility at a site based on information from penetration testing. Kartam N, Flood I, Garrett JH, editors. Artificial neural networks for civil engineers: fundamentals and applications, USA: New York; 1997. p. 185–214.

[18] Ali HE, Najjar YM. Neuronet-based approach for assessing liquefaction potential of soils. Transp Res Rec 1998;1633:3–8.

[19] Najjar YM, Ali HE. CPT-based liquefaction potential assessment: a neuronet approach. Geotech Spec Publ ASCE 1998;1:542–53.

[20] Ural DN, Saka H. Liquefaction assessment by neural networks. Electronic J Geotech Engrg. <http://geotech.civen.okstate.edu/ejge/ppr9803/index.html>.

[21] Juang CH, Chen CJ. CPT-based liquefaction evaluation using artificial neural networks. Comput-Aid Civ Infra Eng 1999;14(3):221–9.

[22] Goh ATC. Probabilistic neural network for evaluating seismic liquefaction potential. Can Geotech J 2002;39(39):219–32.

[23] Javadi AA, Rezania M, MousaviNezhad M. Evaluation of liquefaction induced lateral displacements using genetic programming. Comput Geotech 2006;33:222–33.

[24] Young-Su K, Byung-Tak K. Use of artificial neural networks in the prediction of liquefaction resistance of sands. J Geotech Geoenviron Eng 2006;132(11):1502–4.

[25] Goh ATC, Goh SH. Support vector machines: their use in geotechnical engineering as illustrated using seismic liquefaction data. Comput Geotech 2007;34(5):410–21.

[26] Lanckriet GRG, El Ghaoui L, Bhattacharyya C, Jordan MI. Minimax probability machine. In: Dietterich TG, Becker S, Ghahramani Z, editors. Advances in Neural Information Processing Systems 14. MIT Press: Cambridge: MA; 2002.

[27] Xiangyang M, Taiyi Z. A novel minimax probability machine. Info Tech J 2009;8(4):615–8.

[28] Wang J, Wang ST, Deng ZH, Qi YS. Image thresholding based on minimax probability criterion. Pattern Recogn Artif Intell 2010;23(6):880–4.

[29] Zhou Z, Wang Z, Sun X. Face recognition based on optimal kernel minimax probability machine. J Theor Appl Inf Tech 2013;48(3):1645–51.

[30] Juang CH, Yuan H, Lee DH, Ku CS. Assessing CPT-based methods for liquefaction evaluation with emphasis on the cases from the Chi–Chi, Taiwan, earthquake. Soil Dyn Earthquake Eng 2002;22(3):241–58.

[31] Ku CS, Lee DH, Wu JH. Evaluation of soil liquefaction in the Chi–Chi Taiwan earthquake using CPT. Soil Dyn Earthquake Eng 2004;24:659–73.